Vibrational properties of Re_3N from experiment and theory

Alexandra Friedrich* and Björn Winkler
Geowissenschaften, Goethe-Universität, Altenhöferallee 1, D-60438 Frankfurt a.M., Germany

Keith Refson
Rutherford-Appleton Laboratory, Chilton, Didcot, Oxfordshire OX11 0QX, United Kingdom

Victor Milman
Accelrys, 334 Science Park, Cambridge CB4 0WN, United Kingdom

(Received 27 August 2010; revised manuscript received 28 October 2010; published 17 December 2010)

We report the elastic, electronic, and vibrational properties of hexagonal Re_3N rhenium nitride from experiment and theory using density-functional-theory-based atomistic model calculations. Re_3N was formed at 12 and 20 GPa at about 2000 K in a laser-heated diamond-anvil cell and recovered at ambient conditions. The structural model proposed recently is confirmed by a comparison of the vibrational properties obtained from Raman spectroscopy and from theory, which are in very good agreement. The mode Grüneisen parameters are reported from the pressure-dependent shift of the vibrational modes. The calculated density of electronic states at the Fermi level shows that Re_3N is metallic in the pressure range 0–20 GPa.

DOI: 10.1103/PhysRevB.82.224106 PACS number(s): 63.20.−e, 78.30.−j

I. INTRODUCTION

It is well known that the introduction of smaller atoms such as nitrogen and carbon into interstitial sites in close-packed transition-metal (*TM*) lattices leads to dramatic changes in the physical properties of the compound with respect to that of the metal, such as increasing melting temperatures to nearly 4000 K in some binary *TM* carbides. Numerous binary *TM* borides and carbides have found applications as abrasives or "ultrahigh-temperature ceramics".[1,2] The origin of the unusual properties is the complex bonding found in these compounds, where there are metal-metal, metal-nonmetal, and nonmetal-nonmetal contacts. One of the main approaches in the systematic search for further materials with outstanding properties focuses on the formation of compounds based on metals with high densities of valence electrons, such as rhenium, osmium, and iridium.[3,4] Nitrides and carbides formed with these metals would complement the extensive knowledge available for binary nitrides and carbides formed by transition metals of groups IV-VI (Hf, Ta, W).[5] The known *TM* nitrides and carbides of the remaining period 6 elements (Re, Os, Ir, Pt, Au, Hg) are orthorhombic OsN_2,[6] trigonal IrN_2,[6,7] cubic PtN_2,[7,8] hexagonal Re_2C,[9] and cubic PtC.[10] Recently, we have synthesized two rhenium nitrides, Re_3N and Re_2N, at high pressures and temperatures and characterized them using powder x-ray diffraction, white-beam microdiffraction, and quantum-mechanical calculations based on density-functional theory (DFT).[11] Structural models for the rhenium nitrides were derived from crystal chemical considerations, Rietveld refinement of the rhenium positions, and from DFT. It was found, that N_2 dissociates, like during the formation of, e.g., TaN, TiN, or η-Ta_2N_3.[5,12,13] No N_2 entities are incorporated in the crystal structures as is the case in OsN_2, IrN_2, and PtN_2.[6,7] The crystal structure of Re_3N was described in space group $P\bar{6}m2$ with an *ABB* stacking sequence of the rhenium atoms [Wyckoff positions 2(h) and 1(f)] and the nitrogen atoms occupying Wyckoff position 1(e) between the *BB* layers (Fig. 1).[11] However, in the earlier study no structure-property relations were presented. In this study we present the vibrational properties of Re_3N as derived from Raman spectroscopy and DFT, and also discuss elastic and electronic properties.

II. EXPERIMENTAL DETAILS

Small pieces of rhenium were cut from a pure (>99.98%) rhenium foil with an initial thickness of 25 μm and loaded into holes of 140–160 μm diameter in tungsten gaskets preindented to thicknesses of 38–44 μm in Boehler-Almax diamond-anvil cells. For the thermal insulation compressed KCl plates were placed on top of both diamond anvils. Small pieces of ruby were loaded for pressure determination using the ruby fluorescence method.[14] Nitrogen was loaded at a pressure of 0.18 GPa within a pressure

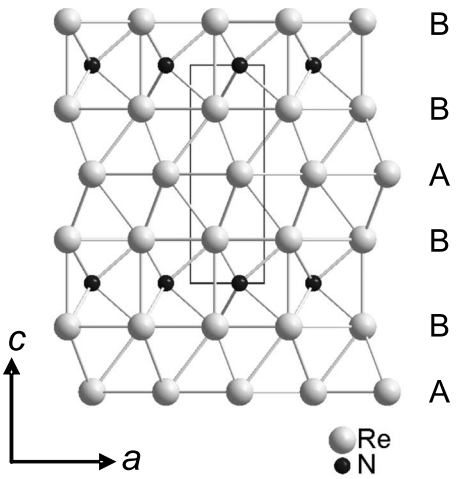

FIG. 1. Crystal structure of Re_3N (space group $P\bar{6}m2$).

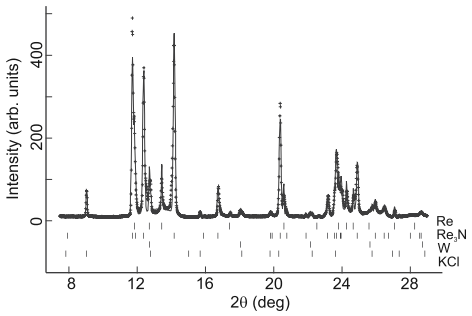

FIG. 2. Powder x-ray diffraction pattern ($\lambda = 0.4959$ Å) showing the presence of Re_3N and Re in a sample recovered to ambient conditions after synthesis. Symbols (+) represent experimental values. The result of the Le Bail fit is shown by the continuous line through the data points. Vertical bars show the positions of the allowed Bragg reflections of the different phases.

vessel as both a reaction compound and a pressure-transmitting medium.

Synthesis experiments were conducted in house at pressures of 12(1) GPa and 20.1(3) GPa by one-sided laser heating with a 100 W ytterbium fiber laser (1.07 μm wavelength) at powers of 20–28 W, which gave temperatures of about 2000 K as estimated from the optical emission of the samples. An exact temperature determination was not possible with the current setup. As the current experiment was aimed to synthesize more material of Re_3N, and not to confirm the stability field of the previous study,[13] this shortcoming had no consequences in the present context. The reaction products were characterized still within the gasket hole after recovering to room conditions by synchrotron powder x-ray diffraction at the Advanced Light Source (ALS, LBNL, Berkeley, beamline 12.2.2). A typical powder-diffraction pattern of one of the samples analyzed shows the presence of both Re_3N and Re within the sample as well as diffraction from the tungsten gasket and the KCl pressure medium (Fig. 2). No Re_2N was observed.

For the micro-Raman measurements, the samples were removed from the gasket hole and put on a glass plate. The KCl thermal insulation was removed and mainly rhenium nitride and rhenium as well as small ruby chips were present. Micro-Raman measurements were then performed on both samples in 180° reflection geometry with a Renishaw Raman spectrometer (RM-1000) equipped with a HeNe laser (633 nm, 50 mW) and a Nd/YAG laser (532 nm, 200 mW). The system was calibrated using the band at 519 cm^{-1} of a silicon wafer.[15] We employed a 20× objective lens. In order to avoid any damage of the sample by the laser radiation, only 10% of the full laser power was applied when using the green Nd/YAG laser. The spectra were recorded at different positions on the samples in the spectral range from 100 to 4000 cm^{-1} and in the limited range of 100–700 *(*or 100–900*)* cm^{-1}, respectively. The latter was selected in order to reduce measurement times and to avoid overexposure of the charge coupled device camera by fluorescence at higher wave numbers during long exposure times. Exposure times varied between 10 and 180 s. The Raman bands were fitted to pseudo-Voigt functions using the program DATLAB.[16]

TABLE I. Lattice parameters of Re_3N from DFT at various calculated pressures.

	Expt.	DFT-PBE			DFT-WuCohen		
p (GPa)	0.0001	0	10	20	0	10	20
a (Å)	2.8105(5)	2.825	2.800	2.777	2.806	2.782	2.761
c (Å)	7.154(2)	7.159	7.115	7.076	7.114	7.072	7.035
c/a	2.545	2.534	2.541	2.548	2.535	2.542	2.548

TABLE II. Elastic stiffness coefficients c_{ij} and bulk modulus B of Re_3N from DFT calculations using the PBE and the Wu-Cohen exchange potentials, respectively. All values are given in gigapascal. The experimentally obtained bulk modulus is 395(7) GPa (Ref. 11).

	c_{11}	c_{33}	c_{44}	c_{12}	c_{13}	B
PBE	662(3)	757(4)	194(1)	207(1)	273(1)	394(1)
WuCohen	691(3)	791(7)	207(1)	220(1)	287(1)	413(1)

III. COMPUTATIONAL DETAILS

DFT calculations were performed using the CASTEP code.[17] The code is an implementation of Kohn-Sham DFT based on a plane-wave basis set in conjunction with pseudopotentials. The plane-wave cutoff was set to 600 eV. All pseudopotentials were ultrasoft.[18] One set of calculations was done by employing the PBE-GGA exchange-correlation functional[19] while in a second set the Wu-Cohen-GGA functional was employed.[19,20] The rhenium pseudopotential is characterized by a core radius of 2.1 a.u. and the 5s and 5p semicore states were treated as valence states. The nitrogen pseudopotential had a core radius of 1.5 a.u. The Brillouin-zone integrals were performed using Monkhorst-Pack grids[21] with spacings between grid points of less than 0.02 $Å^{-1}$. Full geometry optimizations at pressures between 0 and 20 GPa were performed so that forces were converged to 0.004 eV/Å and the stress residual to 0.05–0.15 GPa. Elastic stiffness coefficients were obtained by the stress-strain method and phonons were computed by the finite displacement technique[22] for both phases. Phonon dispersion curves were calculated along the high-symmetry directions in reciprocal space, i.e., from Γ to the A, K, and M points of the Brillouin zone, from 0 to 20 GPa using the PBE-GGA functional and a rectilinear supercell elongated only along the same direction. This method avoids aliasing error only for q vectors in the elongation direction but permits the use of a primitive or small cell in perpendicular directions, avoiding the very high computational cost of a supercell extended in all three directions. It is formally equivalent to the planar force constant method of Ref. 22. The electronic density of states (DOS) was computed from 0 to 20 GPa applying the adaptive smearing technique.[23,24] The PBE-GGA functional and a $36 \times 36 \times 15$ k-point grid were used. The Fermi energy has been rebased to 0 eV.

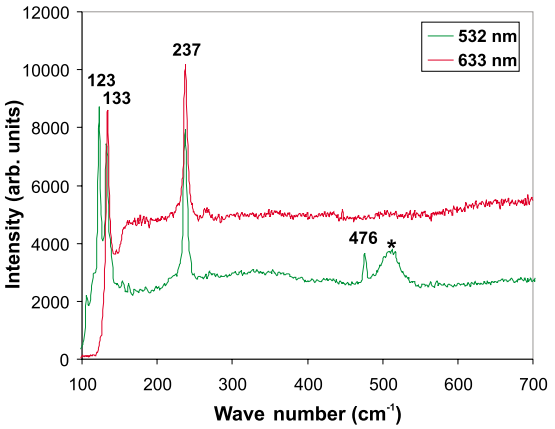

FIG. 3. (Color online) Raman spectra of Re_3N applying a HeNe laser (top, 633 nm, 50 mW) and a Nd/YAG laser (bottom, 532 nm, 20 mW). The broad band indicated by a star is attributed to ruby fluorescence.

IV. RESULTS AND DISCUSSION

Lattice parameters at various pressures obtained from geometry optimizations are given in Table I while the computed elastic stiffness coefficients c_{ij} and bulk modulus B are given in Table II.

The bulk modulus computed from the elastic stiffness coefficients is 394 GPa using the PBE exchange potential and 413 GPa using the Wu-Cohen exchange potential in the calculations. This is in good agreement with the experimental data, where a fit with a second-order Birch Murnaghan equation of state gave a bulk modulus of $B=395(7)$ GPa for Re_3N. Hence, Re_3N is significantly less compressible than rhenium, which has a bulk modulus $B=360-372$ GPa.[25,26] The larger value of c_{33} if compared to c_{11} shows a slightly stiffer behavior of the c axis with respect to the a axis. As there is no pressure-induced structural phase transition and as the atomic positions are constrained by symmetry, the structural compression proceeds via bond compression. The only unconstrained atomic z coordinate ($z=0.198$) of the rhenium atom on Wyckoff position 2(h) does not change at increasing pressure up to 20 GPa within the numerical uncertainty of the calculations.

According to group theory, hexagonal Re_3N has six vibrational modes in the long-wavelength limit: $\Gamma=2E'+2A_2''+1E''+1A_1'$. Four optic modes are Raman active: $\Gamma_{Ra}=2E'+1E''+1A_1'$ and four optic modes are infrared active: $\Gamma_{IR}=2E'+2A_2''$. Typical Raman spectra of Re_3N are shown in Fig. 3. All four Raman-active modes could be measured using a green laser for excitation (Table III). The Raman bands exhibit a sharp linewidth of 3.5–6 cm^{-1}, which is in contrast to the broad band at 510 cm^{-1} with a linewidth of about 30 cm^{-1}. Hence, this broad band is not attributed to Re_3N. It might be due to fluorescence as it is not observed using the red laser with a different wavelength. Only two distinct Raman bands were observed using the red laser for excitation as the lowest frequency mode was cut off by the edge filter at higher frequency compared to the edge filter utilized with the green laser. That the Raman band at 476 cm^{-1} is not observed with the red laser is probably due to its lower intensity.

All of the experimentally measured frequency shifts of the Raman modes coincide very well with the calculated shifts of Raman-active bands from phonon calculations using *ab initio* modeling (Table III). The frequency shifts obtained from calculations using the PBE and the Wu-Cohen exchange potential, respectively, differ only slightly in the low-frequency range by a few cm^{-1} while the difference is up to 25 cm^{-1} at higher frequencies. Consistently, frequencies obtained with the Wu-Cohen exchange functional show larger frequency shifts.

There is only one Raman-active vibrational mode at zero wave vector for pure rhenium (hcp lattice), i.e., the E_{2g} mode at 121 cm^{-1}.[27] The frequency shift of this band is very close to that of the E″ mode of Re_3N with 123 cm^{-1}. This is consistent with the structural model of Re_3N, which is built up by hexagonally close-packed layers of rhenium atoms in an *ABB* stacking sequence. The presence of all Raman-active Re_3N modes in the measured spectra, however, unambiguously demonstrates the presence of Re_3N rather than of pure rhenium. No additional Raman bands were observed that could indicate the presence of N_2 entities within the crystal structure. This confirms, that nitrogen dissociates during synthesis, like during the synthesis of TiN, TaN, and η-Ta_2N_3.[5,12,13]

TABLE III. Phonon frequencies (cm^{-1}) of Re_3N at the Γ point from experiment at ambient conditions and from DFT at various pressures (GPa). Mode Grüneisen parameters γ_i were calculated considering $B_0=394$ GPa for the results using PBE and $B_0=413$ GPa using Wu-Cohen exchange potentials, respectively.

Mode	Expt.	PBE			WuCohen			Activity	γ_i (PBE)	γ_i (Wu-Cohen)
p	0.0001	0	10	20	0	10	20			
E′		0	0	0	0	0	0	Acoustic		
A_2''		0	0	0	0	0	0	Acoustic		
E″	123	121	127	132	125	130	135	Raman	1.79	1.65
E′	133	132	137	141	136	140	144	Raman/IR	1.34	1.21
A_2''		193	205	216	200	211	221	IR	2.35	2.17
A_1'	237	235	244	253	241	250	258	Raman	1.51	1.46
E′	476	479	503	524	495	518	538	Raman/IR	1.85	1.79
A_2''		506	540	570	530	562	590	IR	2.49	2.34

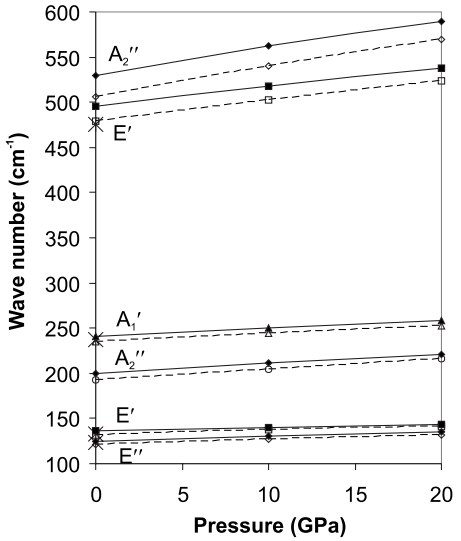

FIG. 4. Frequency shifts of the vibrational modes of Re_3N obtained from DFT calculations using the PBE (dotted lines and open symbols) and Wu-Cohen (solid lines and filled symbols) exchange potentials, respectively. Experimental data (large crosses) are plotted at ambient pressure.

The pressure-induced shifts of the vibrational modes confirm the mechanical stability of Re_3N, which shows no soft mode at any wave vector along the high-symmetry directions in reciprocal space in the range of 0–20 GPa (Figs. 4 and 5, Table III). The mode-Grüneisen parameter γ was calculated for each vibrational mode i according to $\gamma_i = B_0(d\nu_i/dp)/\nu_{i0}$, where B_0 is the bulk modulus at zero pressure (GPa), ν is the frequency (cm^{-1}), p is the pressure (GPa), and ν_{i0} is the frequency of the vibrational mode i at zero pressure (cm^{-1}). The values for B_0 were calculated from the elastic stiffness coefficients (Table II). To be consistent, the values for the bulk modulus and frequency shifts obtained with the same exchange potential (PBE or Wu-Cohen) were used for the calculation of the mode Grüneisen parameters. The mode Grüneisen parameters range between 1.2 and 1.85 for most

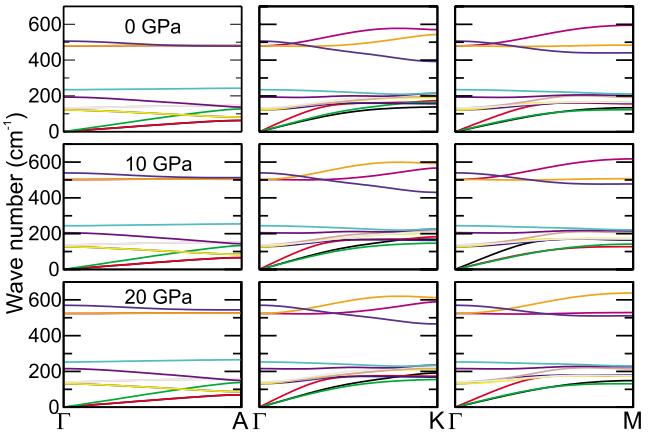

FIG. 5. (Color online) Phonon dispersion curves of Re_3N between 0 and 20 GPa obtained from DFT calculations along high symmetry directions in the Brillouin zone using the PBE exchange potential.

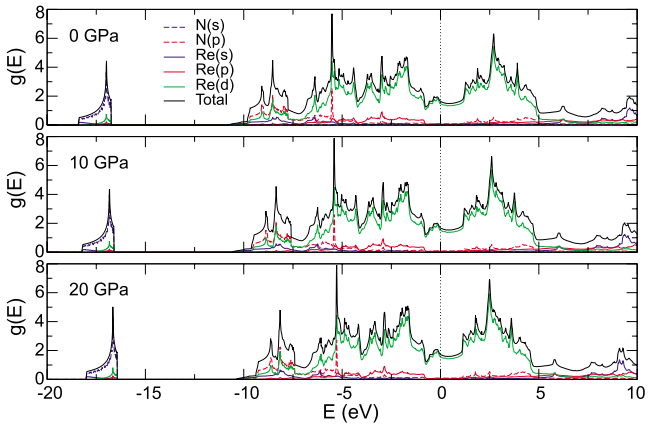

FIG. 6. (Color online) Electronic density of states, g(E), of Re_3N between 0 and 20 GPa obtained from DFT calculations using the PBE exchange potential. The Fermi energy has been rebased to 0 eV.

of the modes, except for two infrared-active A_2'' modes, which show larger mode Grüneisen parameters with $2.17 < \gamma_i < 2.49$ (Table III). For the E_{2g} mode of pure rhenium at 121 cm^{-1} a mode-Grüneisen parameter of 1.8 was reported considering a bulk modulus of 372 GPa.[27] This value is close to γ_i of the E'' mode of Re_3N at 123 cm^{-1} with 1.79 and 1.65 using PBE and Wu-Cohen exchange potentials, respectively.

The calculated electronic DOS of Re_3N shows a large DOS at the Fermi level (Fig. 6). The bulk of the states around the Fermi energy are Re d states. At increasing pressure a slight narrowing of the d bandwidth occurs. Hence, we can conclude, that Re_3N is metallic in the investigated pressure range from 0 to 20 GPa.

V. SUMMARY AND CONCLUSION

In summary, we have verified the proposed structural model for Re_3N as obtained from x-ray diffraction and density-functional theory by studying the vibrational properties. All Raman-active modes, which have been predicted by density-functional theory, could be measured experimentally. The experimentally measured frequencies of the Raman modes coincide very well with the calculated frequencies of Raman-active bands from *ab initio* modeling. Hence, nitrogen dissociates during the synthesis of Re_3N similar to the phase formation of TiN, TaN, and η-Ta_2N_3 from the elements. This is in contrast to the other known *TM* nitrides of period 6 elements with higher atomic numbers, i.e., OsN_2,[6] IrN_2,[6,7] and PtN_2.[7,8]

ACKNOWLEDGMENTS

Financial support from the DFG, Germany, within SPP1236 (Projects No. FR-2491 and No. WI-1232) and the BMBF, Germany (Project No. 05KS7RF1) is gratefully acknowledged. CASTEP calculations were performed on STFC

E-Science facility. The Advanced Light Source is supported by the Director, Office of Science, Office of Basic Energy Science, of the U.S. Department of Energy under Contract No. DE-AC02-05CH11231. A.F. thanks the FOKUS program of the Goethe-university for financial support. We thank A. Woodland (Frankfurt) for access to the Raman spectrometer and S. M. Clark (ALS) for technical support at beamline 12.2.2.

*friedrich@kristall.uni-frankfurt.de

[1] E. Opila, S. Levine, and J. Lorincz, J. Mater. Sci. **39**, 5969 (2004).
[2] Y. D. Blum, J. Marschall, D. Hui, B. Adair, and M. Vestel, J. Am. Ceram. Soc. **91**, 1481 (2008).
[3] R. B. Kaner, J. J. Gilman, and S. H. Tolbert, Science **308**, 1268 (2005).
[4] R. W. Cumberland, M. B. Weinberger, J. J. Gilman, S. M. Clark, S. H. Tolbert, and R. B. Kaner, J. Am. Chem. Soc. **127**, 7264 (2005).
[5] H. O. Pierson, *Handbook of Refractory Carbides and Nitrides* (Noyes, Westwood, New Jersey, 1996).
[6] A. F. Young, C. Sanloup, E. Gregoryanz, S. Scandolo, R. J. Hemley, and H.-k. Mao, Phys. Rev. Lett. **96**, 155501 (2006).
[7] J. C. Crowhurst, A. F. Goncharov, B. Sadigh, C. L. Evans, P. G. Morrall, J. L. Ferreira, and A. J. Nelson, Science **311**, 1275 (2006).
[8] E. Gregoryanz, C. Sanloup, M. Somayazulu, J. Badro, G. Fiquet, H.-k. Mao, and R. J. Hemley, Nature Mater. **3**, 294 (2004).
[9] E. A. Juarez-Arellano, B. Winkler, A. Friedrich, D. J. Wilson, M. Koch-Müller, K. Knorr, S. C. Vogel, J. J. Wall, H. Reiche, W. Crichton, M. Ortega-Aviles, and M. Avalos-Borja, Z. Kristallogr. **223**, 492 (2008).
[10] S. Ono, T. Kikegawa, and Y. Ohishi, Solid State Commun. **133**, 55 (2005).
[11] A. Friedrich, B. Winkler, L. Bayarjargal, W. Morgenroth, E. A. Juarez-Arellano, V. Milman, K. Refson, M. Kunz, and K. Chen, Phys. Rev. Lett. **105**, 085504 (2010).
[12] A. Zerr, G. Miehe, J. Li, D. A. Dzivenko, V. K. Bulatov, H. Höfer, N. Bolfan-Casanova, M. Fialin, G. Brey, T. Watanabe, and M. Yoshimura, Adv. Funct. Mater. **19**, 2282 (2009).
[13] A. Friedrich, B. Winkler, L. Bayarjargal, E. A. Juarez-Arellano, W. Morgenroth, J. Biehler, F. Schröder, J. Yan, and S. M. Clark, J. Alloys Compd. **502**, 5 (2010).
[14] H. K. Mao, J. Xu, and P. M. Bell, J. Geophys. Res. **91**, 4673 (1986).
[15] P. A. Temple and C. E. Hathaway, Phys. Rev. B **7**, 3685 (1973).
[16] K. Syassen, DATLAB, Version 1.38xp, MPI/FKF Stuttgart, Germany, 2005.
[17] S. J. Clark, M. D. Segall, C. J. Pickard, P. J. Hasnip, M. I. J. Probert, K. Refson, and M. C. Payne, Z. Kristallogr. **220**, 567 (2005).
[18] D. Vanderbilt, Phys. Rev. B **41**, 7892 (1990).
[19] J. P. Perdew, K. Burke, and M. Ernzerhof, Phys. Rev. Lett. **77**, 3865 (1996).
[20] Z. Wu and R. E. Cohen, Phys. Rev. B **73**, 235116 (2006).
[21] H. J. Monkhorst and J. D. Pack, Phys. Rev. B **13**, 5188 (1976).
[22] K. Kunc and R. M. Martin, Phys. Rev. Lett. **48**, 406 (1982).
[23] A. J. Morris and C. J. Pickard, LINDOS Version 1.0 User Manual, University College London, 2010.
[24] J. Yates, X. Wang, D. Vanderbilt, and I. Souza, Phys. Rev. B **75**, 195121 (2007).
[25] Y. K. Vohra, S. J. Duclos, and A. L. Ruoff, Phys. Rev. B **36**, 9790 (1987).
[26] R. Jeanloz, B. K. Godwal, and C. Meade, Nature (London) **349**, 687 (1991).
[27] H. Olijnyk, P. Jephcoat, and K. Refson, Europhys. Lett. **53**, 504 (2001).